# POPULATION GENOMIC ANALYSIS OF *CRYPTOCOCCUS* BRAZILIAN STRAINS REVEALS AN AFRICAN TYPE SUBCLADES DISTRIBUTION

Corinne MAUFRAIS[1,2], Luciana de OLIVEIRA[1], Rafael W. BASTOS[3], Frédérique MOYRAND[1], Flavia C. G. REIS[4,5], Clara VALERO[3], Bianca GIMENEZ[4], Luisa J. JOSEFOWICZ[4], Gustavo H. GOLDMAN[3], Marcio L. RODRIGUES[4,6] and Guilhem JANBON[1]*

[1] Institut Pasteur, Unité Biologie des ARN des Pathogènes Fongiques, Département de Mycologie, F-75015, Paris, France
[2] Institut Pasteur, HUB Bioinformatique et Biostatistique, C3BI, USR 3756 IP CNRS, F-75015, Paris, France
[3] Departamento de Ciências Farmacêuticas, Faculdade de Ciências Farmacêuticas de Ribeirão Preto, Universidade de São Paulo, Ribeirão Preto,Brazil
[4] Instituto Carlos Chagas, Fundação Oswaldo Cruz (FIOCRUZ), Curitiba, Brazil
[5] Centro de Desenvolvimento Tecnologico em Saude (CDTS-Fiocruz), Brazil
[6] Instituto de Microbiologia Paulo de Góes (IMPG), Universidade Federal do Rio de Janeiro, Rio de Janeiro, Brazil

* Corresponding author
[1,2] Both authors should be considered as first authors

**Abstract**

The genome of a large number of *Cryptococcus neoformans* isolates has been sequenced and analyzed in recent years. These genomes have been used to understand the global population structure of this opportunistic pathogen. However, only a small number of South American isolates have been considered in these studies, and the population structure of *C. neoformans* in this part of the world remains evasive. Here, we analyzed the genomic sequences of 53 Brazilian *Cryptococcus* isolates and deciphered the *C. neoformans* population structure in this country. Our data reveal an African-like structure that suggesting repeated and privileged intercontinental transports from Africa to South America. We also identified a mutator phenotype in one VNBII Brazilian isolate, exemplifying how fast-evolving isolates can shape the *Cryptococcus* population structure. Finally, phenotypic analyses revealed wide diversity but not lineage specificity in the expression of classical virulence traits within the set of isolates.

The current classification identifies seven *Cryptococcus* species pathogenic for humans, which are responsible for 180,000 deaths every year in the world (HAGEN *et al.* 2015; RAJASINGHAM *et al.* 2017). *C. neoformans* and *C. deneoformans* represent the *neoformans* group of species, whereas the gattii group of species comprises *C. gattii*, *C. deuterogattii*, *C. tetragattii*, *C. decagattii*, and *C. bacillisporus* (HAGEN *et al.* 2015). *C. neoformans* is the most common species in clinical settings, representing more than 95% of the clinical isolates (KWON-CHUNG *et al.* 2014; JANBON *et al.* 2019). This species affects mostly immunocompromised patients in whom it provokes meningoencephalitis. Other species, such as *C. gattii*, can be primary pathogens and cause pulmonary infections (KWON-CHUNG *et al.* 2014). *C. neoformans* is thought to be acquired very early in life and can stay in a dormant state for years, probably in alveolar macrophages (GARCIA-HERMOSO *et al.* 1999; ALANIO 2020). As soon as a defect in the cellular immunity appears, yeasts can multiply, reach the central nervous system, and induce meningo-encephalitis, which is invariably deadly if untreated.

*C. neoformans* strains are ubiquitous in the environment and have been isolated from all continents except Antarctica. Similarly, although strains of the *gattii* group of species have been long considered to be geographically restricted to tropical and subtropical regions and typically associated with *Eucalyptus* trees, they have emerged as a primary pathogen in western Canada and United States of America (KIDD *et al.* 2004). Both species can live in a broad range of ecological habitats and have been commonly isolated from soil, guano, decaying wood, fruits, and insects (LIN AND HEITMAN 2006). Pigeons (*Columba livia*) are vectors for the worldwide dissemination of *Cryptococcus*. Indeed, dry pigeon guano seems to be an ideal environment for *C. neoformans* development and is commonly infected with this fungus. Nevertheless, pigeons are usually not infected by *C. neoformans* because their body temperature is too high (42.5°C) for its growth and disease development (JOHNSTON *et al.* 2016).

All *neoformans* and *gattii* species are haploid species with two possible mating type alleles (*MAT***a** and *MATα*) and a bipolar mating system. Efficient sexual reproduction has also been described in the laboratory. Nevertheless, *C. neoformans MAT***a** strains are rare in clinical and environmental isolates with the exception of some places in Africa (KWON-CHUNG AND BENNETT 1978; LITVINTSEVA *et al.* 2003). In addition, it has been reported that 8% of the population of *C. neoformans* strains are diploid (LIN *et al.* 2009). Diverse hybrid strains have also been isolated from environmental and clinical sources. The most common are AD hybrids, which are produced by hybridization of *C. neoformans* with *C. deneoformans* isolates. In addition, rare cases of *gattii*/*neoformans* hybrids have been reported (BOVERS *et al.* 2008; AMINNEJAD *et al.* 2012). Nevertheless, population structure analysis suggested that the different *neoformans* and *gattii* populations are largely clonal with a limited degree of recombination (LITVINTSEVA *et al.* 2005; BUI *et al.* 2008; LITVINTSEVA AND MITCHELL 2012).

Historically, these analyses were first based on serotyping, which was first replaced by PCR-based characterization (RAPD, AFLP, mating type analysis) of the isolates and then by sequencing of a defined set of genes by multilocus sequencing typing (MLST) (RUMA *et al.* 1996; BOEKHOUT *et al.* 2001; MATSUMOTO *et al.* 2007; MEYER *et al.* 2009a). Originally, five *neoformans* molecular subtypes were thus defined (VNI, VNII, VNIV, VNIII, and VNB) (MEYER *et al.* 2009b). The new species definition includes VNI, VNII, and VNB within *C. neoformans*, VNIV within *C. deneoformans*, and VNIII as *C. neoformans*/*C. deneoformans* hybrids. VNI is the most common *C. neoformans* molecular subtype and has a global distribution. The VNB subtype was discovered in Africa and has a genetically variable population, 10% *MAT***a** strains, which are very rare in all other studied populations (LITVINTSEVA *et al.* 2003). The VNB clade includes strains isolated from the endemic mopane tree (*Colophospermum mopane*), whereas strains isolated from pigeon excreta in the same area had the VNI molecular type, which is shared by most strains globally. This observation supported the "out of Africa" hypothesis in which few

of these strains would have adapted their biology to multiply in pigeon to achieve global dispersion (LITVINTSEVA *et al.* 2011; LITVINTSEVA AND MITCHELL 2012).

More recently, the improvement of sequencing technologies and bioinformatics tools allowed analysis of whole genome sequences, revealing more details in the structure and global geographical distribution of the *Cryptococcus* populations together with the identification of additional clades and subclades (FARRER *et al.* 2019). Most of these studies focused on *C. neoformans*, with >1000 *C. neoformans* genome sequences analyzed in four studies (DESJARDINS *et al.* 2017; RHODES *et al.* 2017b; VANHOVE *et al.* 2017; ASHTON *et al.* 2019; ERGIN *et al.* 2019). Through these efforts, the VNB clade has been separated into the VNBI and VNBII subclades, which have different resistance to oxidative stress and a different ability to produce melanin (DESJARDINS *et al.* 2017; VANHOVE *et al.* 2017). The VNI clade has been separated into a number of subclades with three phylogenetic groups representing the majority of the studied isolates (RHODES *et al.* 2017b; ASHTON *et al.* 2019). Surprisingly, only 11 haploid strains isolated in South America were included in these studies. This small number conflicts with the relevance of South America as a source of genetic diversity in the *gattii* isolates (ENGELTHALER *et al.* 2014). Up until now, the only analysis of *C. neoformans* population structure in South America has been an MLST analysis that concluded that subtype ST93 was the most prevalent among strains isolated from HIV patients in Southeastern Brazil with a low level of recombination (FERREIRA-PAIM *et al.* 2017). Similarly, few phenotypic analyses that include South American isolates have been published, and a recent analysis of virulence factor expression within Brazilian *Cryptococcus* clinical isolates does not include any sequencing or molecular typing analysis (DE SOUSA *et al.* 2020). In the present study, we analyzed the phenotypes and genome sequences of 53 Brazilian isolates, revealing very high phenotypic diversity within *Cryptococcus* isolates and a subclade distribution that suggests several waves of *Cryptococcus* introduction from Africa to South America.

## Material and Methods

### Strains used in this study

Strains 2B, 2C, 2D, 4C, 7, 33A1, 54A1, 56A1, 68B1, 69A1, 81A1, 96A1, 106A1, 144A1, 151A1, 176A1, 3Pb3, 5Pb2, 19Pb4, 23Pb2, 32Bp1, and RR 2605 were isolated from Northern Brazil (DAL PUPO *et al.* 2019) and kindly donated by Dr. Halan Dal Pupo. Strains Cn201, Cn359, Cn894, Cn14HC, and Cn201 were obtained from the culture collection of the Central Hospital of the University of São Paulo. All other strains were obtained from the Collection of Pathogenic Fungi available at Fiocruz. No genomic information was available for any of these isolates before the present study.

*Read alignment, variant detection, and ploidy analysis*

Illumina reads were aligned to the *Cryptococcus* reference genomes using Minimap2 aligner v. 2.9 (LI 2018) with "-ax sr" parameter. BAM files were sorted and indexed using SAMtools (LI *et al.* 2009) version 1.9. Picard version 2.8.1 (http://broadinstitute.github.io/picard) tools were used to identify duplicate reads and assign correct read groups to BAM files. SAMtools version 1.9 and Picard version 2.8.1 were then used to filter, sort, and convert SAM files and assign read groups and mark duplicate reads. Single-nucleotide polymorphisms (SNPs) and insertion/deletion (indel) positions were called using Genome Analysis Toolkit version 3.6 with ploidy=1 according to the GATK Best Practices. HaploScore parameters used to filter SNPs and indels included VariantFiltration, QD <2.0, LowQD, ReadPosRankSum<-8.0, LowRankSum, FS >60.0, HightFS, MQRankSum<-12.5, MQRankSum, MQ <40.0, LowMQ, and HaplotypeScore >13.0. Phyml version 20120412 (GUINDON *et al.* 2010) with the GTR, NNIs substitution model was used to infer phylogenetic relationships between the isolates using the different dataset of confident SNPs. To examine variations in ploidy across the genome, the sequencing depth at all positions was computed using SAMtools (LI *et al.* 2009), and then the average depth was computed for 1-kb windows across the genome.

### MAT locus determination

The mating type of Brazilian isolates was determined as previously published (RHODES *et al.* 2017b). Briefly, Illumina reads were aligned using BWA-MEM to the mating-type locus sequences [AF542529.2 and AF542528.2]. Computed average depths at the *SXI* and *STE20* loci using SAMtools mpileup were used to determine the mating type.

**Population inference by fastSTRUCTURE**

We used fastStucture (RAJ *et al.* 2014) to identify admixture in the dataset from K=2 to K=4. After K=4, clusters with the highest number of isolates were split into sub-clusters, which likely reflects an issue due to the number of isolates within clusters rather than true biological significance.

*Drug susceptibility testing*

The minimum inhibitory concentration (MIC) of fluconazole (FLC) (Sigma-Aldrich) was determined as described by M27- A3 (INSTITUTE 2017).

**Titan cell production**

Titan cell (TC) production was evaluated as described by Dambuza et al., 2018 with some modifications (DAMBUZA *et al.* 2018). The strains were cultivated in yeast peptone dextrose (YPD) agar (1% yeast extract, 2% bacto-peptone, 2% glucose, 2% bacto-agar) for 48h at 30°C. A single colony was transferred to 5 mL YNB without amino acids (Sigma Y1250) prepared according to the manufacturer's instructions plus 2% glucose. After incubation overnight at 30°C and 200 rpm, $1X10^3$ cells/mL were inoculated into 5 mL 1xPBS (phosphate buffer solution) + 10% heat-inactivated (HI) fetal calf serum (FCS) and incubated for 72 h at 37°C, 5% $CO_2$. We visualized the cells microscopically without any staining, and 50 cells were measured. TC were considered body cells (without the capsule) with a diameter >10 µm. The experiment was repeated twice.

*Capsule staining*

Fungal cells were cultivated in YPD agar for 24 h at room temperature. Single colonies were transferred by sterile loop to the wells of a 96-well plate, each containing 200 µL of Roswell

Park Memorial Institute (RPMI) medium at a final cell density of $10^7$ yeast/mL. The plates were incubated for an additional 24 h at 37°C in 5% $CO_2$ and centrifuged to separate the cells from the supernatants. The supernatants were stored for GXM analysis, and the cells were washed twice in PBS for further fixation in 4% paraformaldehyde for 1 h at room temperature. Yeast cells were then blocked (1% bovine serum albumin [BSA] in PBS for 1 h at 37°C) and incubated with the 18B7 anti-GXM monoclonal antibody (CASADEVALL *et al.* 1992) (mAb 18B7; 10 µg/mL for 1 h at 37°C), a kind gift from Dr. Arturo Casadevall (Johns Hopkins University). The cells were washed and incubated with an Alexa Fluor 488-conjugated secondary antibody (10 µg/mL for 1 h at 37°C; Invitrogen, USA). The cells were finally stained with calcofluor white (5 µg/mL for 1 h at 37°C; Invitrogen, USA). Alternatively, the cells were counterstained with India ink for capsular visualization. The cells were visualized on a Leica TCS SP5 confocal microscope or analyzed with a FACS Canto II flow cytometer. Data were processed with the FACSDiva software, version 6.1.3.

**Data availability**

All sequence data from this study have been submitted to GenBank under the SRA identification no. SUB8968088 (http://www.ncbi.nlm.nih.gov/SRA).

## Results

### Description of the origin of the Brazilian isolates

We selected 53 *Cryptococcus* Brazilian isolates, of which 12 were classified as *C. gattii* and 41 as *C. neoformans.* More than 41% (n=22) were environmental and 36% (n=19) were clinical isolates. The origin of the isolate was unknown for the remaining 23% (n=12). Twenty-one strains were isolated from pigeon excreta in Northern Brazil (DAL PUPO *et al.* 2019), 28 strains were obtained from the culture collections available at Fiocruz, and 4 were acquired from the Central Hospital of the University of São Paulo (Table S1).

### Genome characterization

Whole genome sequencing was performed for each of the 53 Brazilian isolates considered in this study. Between 2.7 and 10.9 million 100-nt paired-end reads were obtained and aligned to eight *Cryptococcus* reference genomes using Minimap2 (LI 2018) (Table S1). Reference genomes were *C. neoformans* strain H99 (JANBON *et al.* 2014), *C. deneoformans* strain JEC21 (LOFTUS *et al.* 2005; GONZALEZ-HILARION *et al.* 2016), *C. deuterogattii* strain R265 (YADAV *et al.* 2018), *C. gattii WM276*, *C. bacillisporus* strains CA1280 and CA1873, *C. decagattiii* strain AFLP10, and *C. tetragattii* strain IND107 (BASENKO *et al.* 2018). Of the 53 isolates, 40 were identified as *C. neoformans* with >80% of the reads aligning to the H99 genome (<40% of reads could be aligned to any other reference genome). Among the 13 remaining isolates, 8 were *C. deuterogattii* and 5 were *C. gattii* (Table S1). Of note, we found that strain Cg366, which was previously identified as *C. gattii*, is actually a *C. neoformans* isolate. Strains Cn201 and Cn894, which were previously considered to be *C. neoformans*, were identified as *C. deuterogattii* isolates.

In order to determine mating type, we compared the number of reads aligned to the *STE20a*, *STE20alpha*, *SXI1*, and *SXI2* genes of the corresponding species. These analyses revealed that

all strains were *MATα*, confirming the overwhelming dominance of this mating type in clinical and environmental isolates observed in most areas in the world (DESJARDINS *et al.* 2017).

The analysis of the read alignment profiles provided insight into possible large duplications or aneuploidies. All *C. neoformans* strains displayed an even alignment profile, suggesting that they are haploid. However, we observed a duplication of the end of the chromosome 1 in three strains (Cn160, Cn161 and Cn186)) (left side in Figure 1). The strain Cn161 appears to have additional duplications within the chromosome 8. Similar patterns were observed in the eight *C. deutogattii* isolates, with two isolates (Cn201 and Cn894) displaying a duplication of a region located in the chromosomes 8 and 13, respectively. In contrast, all five *C. gattii* isolates displayed an even alignment profile, suggesting that all are haploid (data not shown).

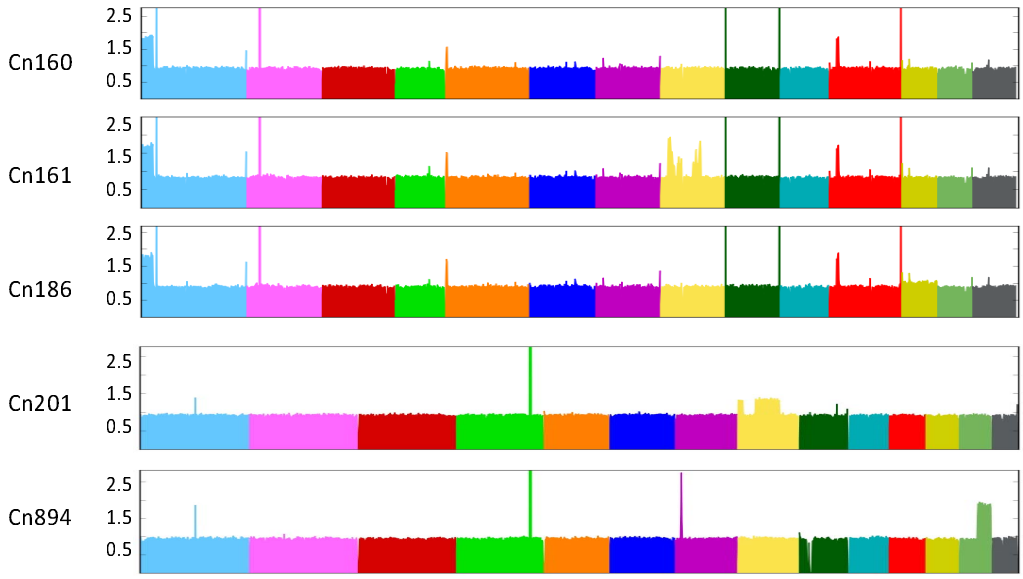


Figure 1. Large segmental duplications within the genomes of Brazilian isolates were revealed after aligning sequencing reads to the *Cryptococcus* reference genomes.

**Phylogenetic analyses**

To obtain insight into the population structure of the Brazilian *C. neoformans* isolates, we constructed a phylogenetic tree including 352 isolates considered in previous studies (DESJARDINS *et al.* 2017; RHODES *et al.* 2017b; ASHTON *et al.* 2019) that encompass all VNI and

VNB subclades (Table S2). We also included 10 VNII isolates as the outgroup to root the tree (DESJARDINS *et al.* 2017; RHODES *et al.* 2017b; ASHTON *et al.* 2019). Overall, 945,565 variable positions were used to construct the tree presented in Figure 2A.

*VNB strains*

Whereas the vast majority (92.5%, n=37) of the *C. neoformans* Brazilian isolates belonged to the VNI clade, we also identified one VNB strain of the VNBII subclade (Cn225). Two other Brazilian isolates (Cn216 and Cn14HC) appear to be associated with the VNBI and VNBII clades, respectively, but with a close-to-the-root long branch (Figure 2A). Accordingly, the number of variant positions compared to the H99 reference genome was slightly higher in these two strains than in the other VNB strains (Figure 2B). As previously reported, analysis of the population using *fastSTRUCTURE* (k=4) (RAJ *et al.* 2014) readily separated VNI, VNII, VNBI, and VNBII strains (DESJARDINS *et al.* 2017) into four independent populations (Figure 2C). As expected, this analysis showed that the two Brazilian outlier strains (Cn216 and Cn14HC) are associated with the VNBI and VNBII clades, respectively.

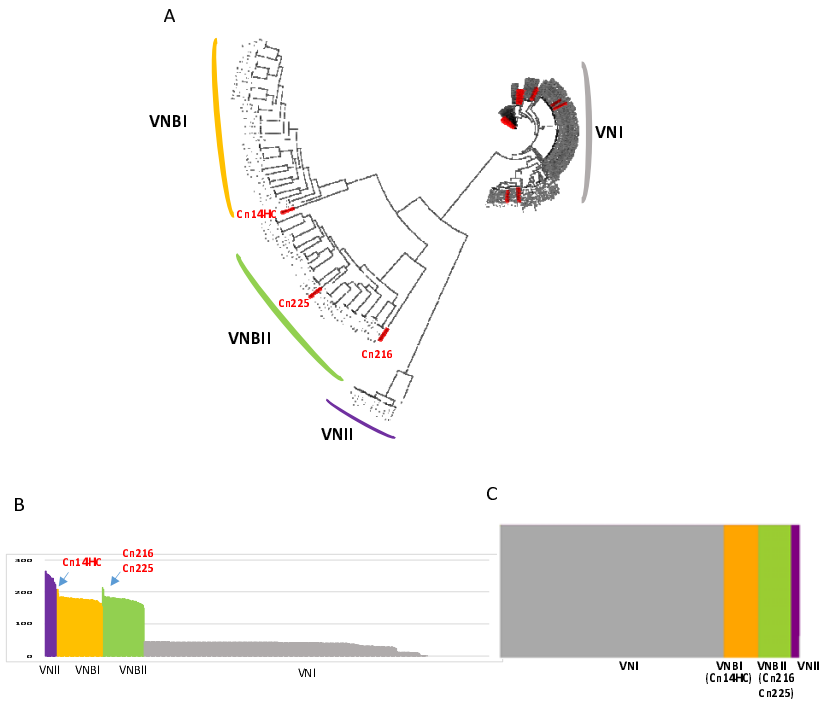


Figure 2. (A) Phylogenetic tree generated by iTOL v5 using *C. neoformans* genome sequences. The Brazilian isolates are indicated in red. The two Brazilian outlier isolates are shown. (B) Number of variant positions within the genomes of the different strains analyzed in this study. (C) Results of the structure analysis (k=4) suggesting VNBI and VNBII origin for the two Brazilian outlier strains (CnH14C and Cn216, respectively).

Because VNI/VNB and VNII/VNB hybrids have been previously reported within African isolates (RHODES *et al.* 2017b), we sought to compare their phylogenetic position with the two outlier Brazilian strains. We first redrew a phylogenetic tree including six of these strains (the VNII/VNB strain MW-RSA852 and four VNI/VNB strains Bt125, Bt131, Bt162, and Bt163) (Figure S1). As previously published, the African hybrid strains are also positioned at the root of the VNB and VNII branches, respectively. We then performed principal component analysis (PCA) including this set of hybrid strains. As previously published, this analysis readily separated strains positioned at an intermediary position between the defined clades (Figure 3) (DESJARDINS *et al.* 2017). Like most African VNI/VNB hybrids, the Bt163 strain was positioned between VNI and VNBII, suggesting that it is a hybrid of strains of these two clades. Of note,

the VNI/VNB strain Bt125 has an intermediary position between the VNBI, VNBII, and VNI lineages (Figure 3).

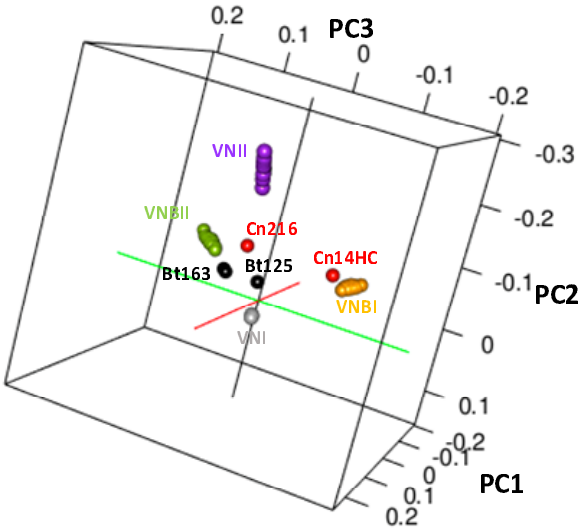


Figure 3. Principal component analysis revealing the intermediary position of the Brazilian outlier strains. VNI/VNB hybrid strains (RHODES *et al.* 2017b) have been added to this analysis. The position of the hybrid (black) and of the two Brazilian outlier strains (in red) is indicated.

The two outlier Brazilian strains are positioned between the VNBI and VNBII isolates, suggesting that they are not VNB/VNI hybrids. In agreement with the location of these strains in the phylogenetic tree, this analysis showed that the Cn216 strain is closer to VNBII isolates whereas the Cn14HC strain is closer to VNBI isolates. According to these results, Cn216 and CnH14C could be either VNBI/VNBII hybrids or evolved VNBI and VNBII isolates, respectively. In order to test these two hypotheses, we first determined the position and number of SNPs specific to each clade (Figure 4A,B). This analysis revealed that the number of clade-specific SNPs was equivalent for each clade with an even distribution along the H99 reference genome. Of note, the VNBI clade appear to have fewer clade-specific SNPs, which might be related to the previously reported loss of diversity in this lineage (DESJARDINS *et al.* 2017).

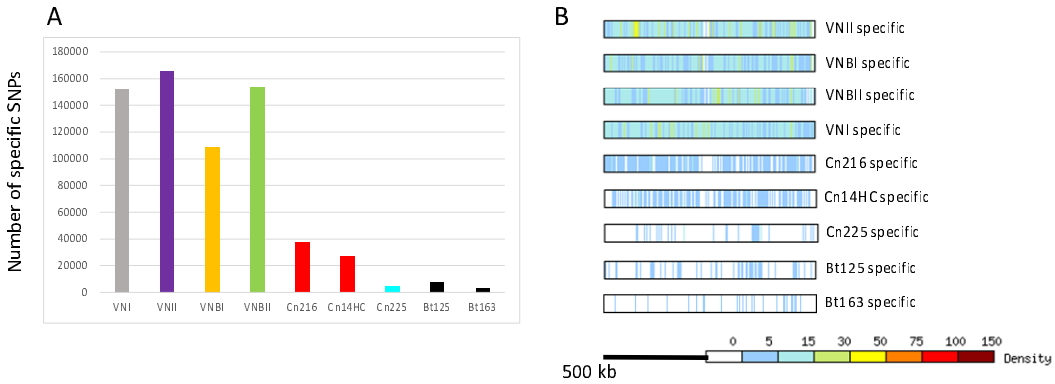


Figure 4. (A) Number of specific SNPs in each clade and in the two Brazilian outlier strains (Cn216 and Cn14HC). The Brazilian VNBII strain Cn225 and the hybrid strains Bt125 and Bt163 (RHODES *et al.* 2017b) were used as controls. (B) Density and position of the clade-specific SNPs on the H99 reference genome. The results obtained with the chromosome 14 are presented.

We reasoned that we could determine the origins of the SNPs in the two outlier Brazilian strains by comparing their positions with clade-specific SNPs (Figure 5). We compared the position of Cn216 and Cn14HC SNPs (n=213,915 and n=207,438, respectively) with the VNI-, VNII-, VNBI-, and VNBI-specific SNPs and plotted the common positions in the H99 reference genome. As a control, we performed the same analysis with the VNBII Brazilian strain Cn215 (n=207,639 SNPs).

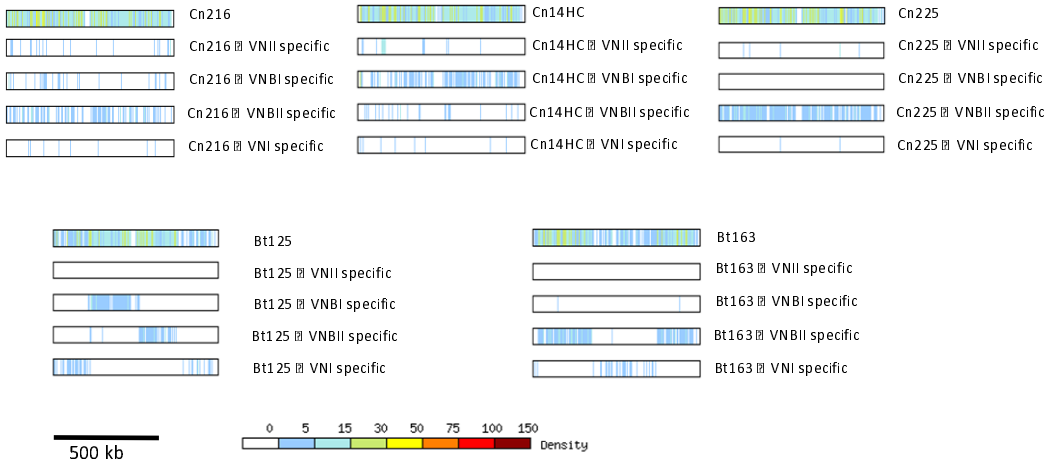


Figure 5. Origin of the SNPs in the Brazilian outlier strains (Cn216 and Cn14HC). SNP positions shared between the clade-specific SNPs were identified and plotted on each chromosome. Chromosome 14 is presented as an example. Results obtained with the Brazilian VNBII Cn225 and the African VNB/VNI hybrid strains Bt125 and Bt163 (RHODES *et al.* 2017b) are shown as controls.

This analysis revealed that the Brazilian outlier strains Cn214 and Cn14HC mostly share SNP positions with the VNBII- and VNBI-specific SNPs, respectively, confirming that they belong to these respective lineages. We observed an even distribution of these SNPs along the chromosomes with no sign of a recent recombination event between the VNBI and VNBII lineages. As expected, a similar result was obtained with the Brazilian VNBII isolate Cn225. In contrast, the African VNB/VNI hybrid Bt163 displays a SNP distribution common to the clade-specific SNPs, supporting a recent recombination event between a VNBII and VNI strain and thus confirming the PCA results and previously published results (RHODES *et al.* 2017b). For the Bt125 strain, the SNP pattern was more complex than previously published, suggesting a triple VNBI/VNBII/VNI origin for this strain, in agreement with the intermediary position of this strain observed by PCA (Figure 3). Overall, these analyses suggest that the Cn214 and CnH14C isolates belong to the VNBII and VNBI clades, respectively, with no sign of recombination with another clade. Yet, the number of the SNPs unique to these two strains (n=37,236 in Cn216 and n=26,925 in CnH14C) is much higher than in the VNBII Brazilian strain Cn225 (n=4788) and in the two VNI/VNB African hybrids (n=7485 in Bt125 and n=3511 in Bt163) (Figure 4A). These strain-specific SNPs are evenly distributed along the H99 reference genome (Figure 4B). This SNP pattern may be due to an ancient separation of these strains from most other strains of their respective clades or a recent but rapid evolution of their genome sequences due to an increased mutation rate.

In order to test these hypotheses, we compared the mutation rates in both Cn216 and Cn14HC by observing the appearance of spontaneous 5-fluorocytosine (FU)-resistant colonies in fluctuation assays (BOYCE *et al.* 2017; BILLMYRE *et al.* 2020). We included the reference strain KN99α and the Brazilian VNBII strain Cn225 as controls. The mutation rate of Cn14HC was higher than those of Cn225 and KN99α (Figure 6). In contrast, the mutation rate in Cn216 was

not significantly different from that of the Cn225 (VNBII). Similar results were obtained when 5-FAO selection was used (Figure S2).

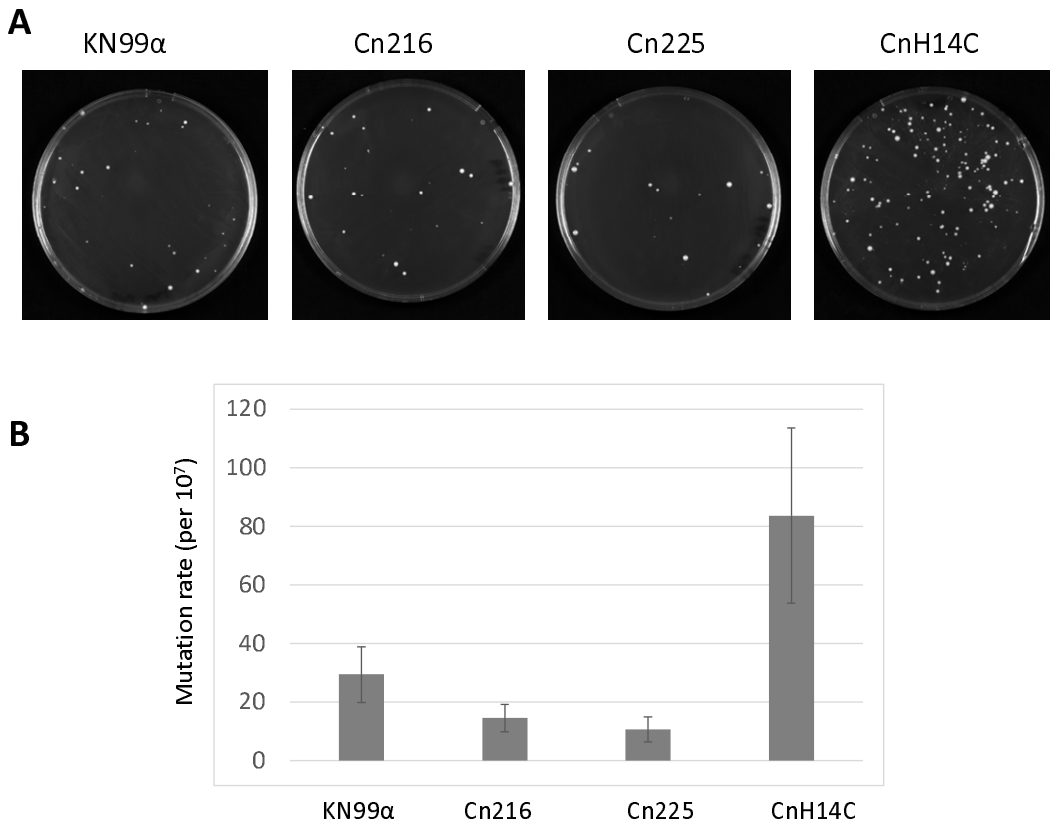


Figure 6. CnH14C display an elevated mutation rate. (A) Spontaneous 5-FU–resistant colonies in a standard wild type (KN99α) isolate and three Brazilian isolates (Cn216, Cn225, and CnH14C). (B) Quantitative assessment of mutation rates in the four strains using fluctuation analysis of the spontaneous resistance to 5-FU. The Lea-Coulson method of the median was used to estimate the number of mutations from the observed values of mutants from 10 independent, parallel cultures (FOSTER 2006; GILLET-MARKOWSKA *et al.* 2015). Error bars indicate 95% confidence intervals.

Strains with mutations in the mismatch repair pathway associated with a mutator phenotype have been observed both in *C. deuterogattii* (BILLMYRE *et al.* 2017) and *C. neoformans* clinical isolates (BOYCE *et al.* 2017; RHODES *et al.* 2017a). Although experimental in vitro analyses suggested that only *MSH2*, *MLH1*, and *PMS1* play a major role in regulating the mutation rate in *C. neoformans* (BOYCE *et al.* 2017), recurrent strain evolution analysis suggested that *MSH5* and *RAD5* could also influence strain evolution in patients (RHODES *et al.* 2017a). Given that we

did not identify Cn14HC-specific nonsense, we looked at the Cn14HC-specific SNPs responsible for non-conservative mutations in these mismatch repair genes. Interestingly, two of these genes contain mutations specific to Cn14HC: *PMS1* (CNAG_07955) encodes a protein with a S483P mutation and *RAD5* (CNAG_04733) encodes a protein with a P332S mutation. In contrast, we did not identify specific SNPs responsible for a change in any of these proteins in Cn216 or Cn225.

Overall, our results suggest that CnH14C possesses a mutator phenotype associated with specific mutations in two mismatch repair genes. This CnH14C mutator phenotype has resulted in rapid evolution and could explain its position in the phylogenic tree. In contrast, Cn216 might be the result of a long evolution independent of the African VNBII strain due to an ancient geographical separation.

*VNI strains*

As stated above, nearly all *C. neoformans* strains in this collection belong to the VNI clade, mostly within the VNIa subclade. Only two strains were identified as VNIb and none were identified as VNIc. Interestingly, the second major lineage within the VNIa Brazilian isolates was VNIa_Y, encompassing 27.5% (n=10) of strains. All of these strains were isolated from pigeon droppings in Northern Brazil. These are the first VNIa_Y strains isolated outside of Africa; previous strains, all of which originated in the environment, were isolated in Botswana, Malawi, and Uganda (ASHTON *et al.* 2019). The structure of the Brazilian VNIa strain resembles that of the African strain. Approximately 45% of the VNIa strains are of the VNIa_93 lineage, similar to previous observations in Ugandan isolates (ASHTON *et al.* 2019). Similar to previous reports for African countries, only 2 of the Brazilian isolates were of the VNIa_5 subclass and no VNIa_4 strains were identified, confirming that these two subclasses are specifically enriched within Southeast Asia isolates (ASHTON *et al.* 2019).

Phylogenetic trees constructed using only the VNIa subclades revealed a clear geographical clustering of the strains (Figure 7), suggesting that the current subclade organization of *C. neoformans* isolates predates the dissemination into South America. However, the existence of unclustered VNI-93 Brazilian isolates suggests multiple intercontinental isolate transfers.

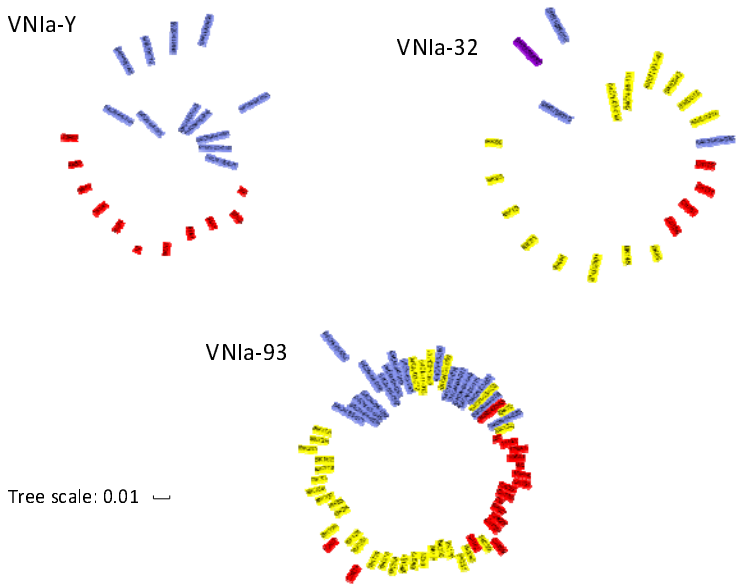


Figure 7. Phylogenetic trees of the VNIa subclades as visualized by ITOL revealed geographic clustering. The Brazilian, African, and South Asian isolates are labelled in red, blue, and yellow respectively. The Indian isolates are labelled in purple.

**Phenotypic analyses**

We next characterized the Brazilian strains at a phenotypic level. We focused our analysis on virulence-associated phenotypes and drug resistance. All strains grew well at 30°C, and only *C. gattii* strain Cg187 and *C. neoformans* VNIa_Y strain 3Pb3 exhibited a growth defect at 37°C (Figure S3). Similarly, most of these *Cryptococcus* isolates demonstrated a low MIC for fluconazole (Table S3), with a $MIC_{50}$ of 2 µg/mL and $MIC_{90}$ of 8 µg/mL. The clinical isolate Cn191 (VNIa_93) and the environmental isolate 151A1 (VNIa_Y) showed the highest MIC values (8.0 µg/mL).

Exportation of GXM, a major capsular antigen, and capsule formation are essential for the *Cryptococcus* virulence. We analyzed multiple aspects of capsule formation in Brazilian

isolates, including capsular morphology, serological reactivity, and extracellular concentration of GXM. Capsule morphology was examined by fluorescence microscopy after incubation of the cells with an antibody to GXM for capsule visualization and calcofluor white for cell wall staining. Alternatively, the capsule was counterstained with India ink for visualization of the capsule by light microscopy. This analysis revealed formidable heterogeneity at morphological and serological levels (Figure 8).

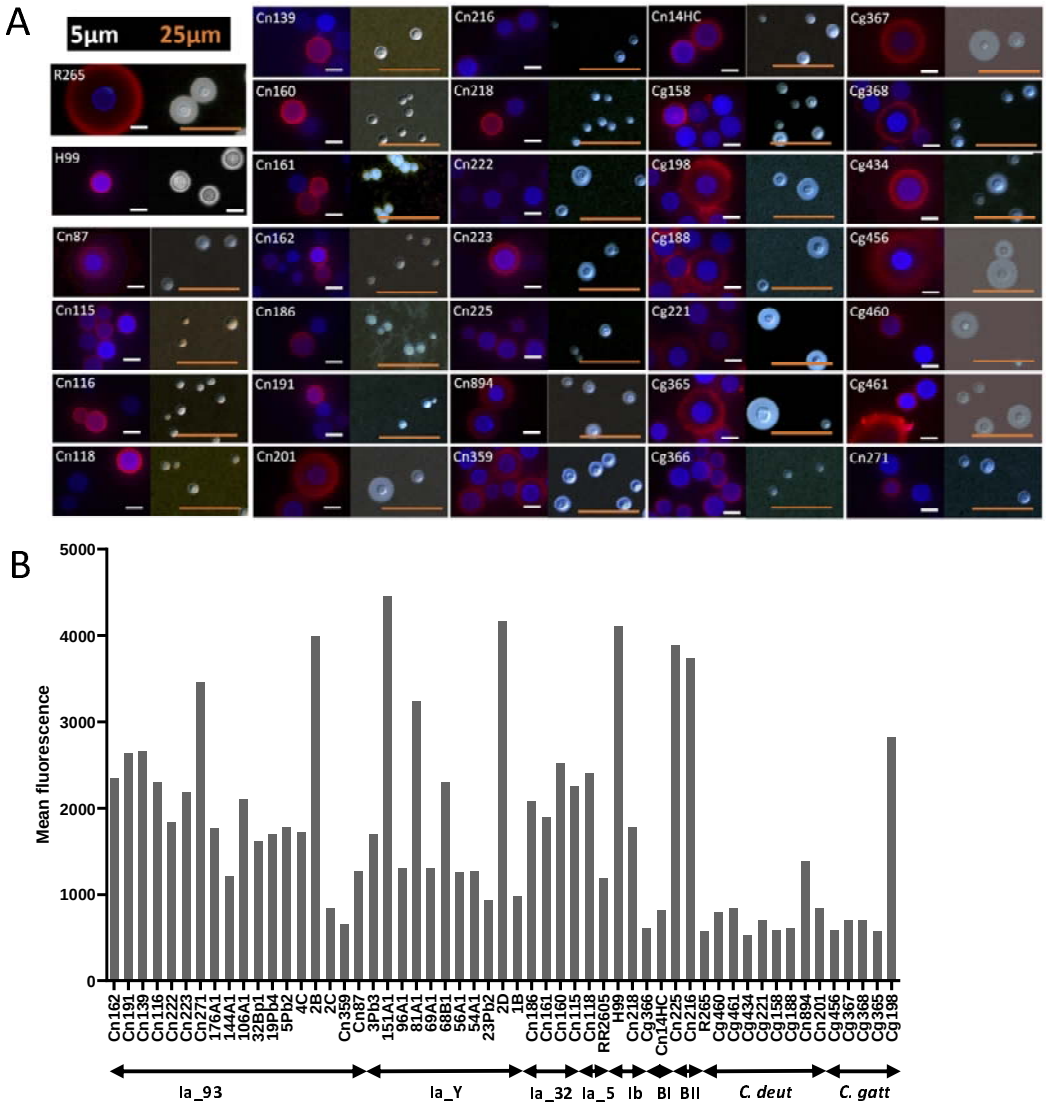


Figure 8 (A) Microscopic analysis of the cell surface of the Brazilian isolates. R265 and H99 are standard cryptococcal isolates that were used as reference in this assay. For each isolate, fluorescence panels are shown on the left and India ink counterstaining is shown on the right. Red fluorescence indicates capsule staining with the mAb 18B7 antibody and blue fluorescence represents cell wall staining. Images are illustrative of two independent analyses that

produced similar results. Corresponding data for the Northern Brazil isolates have been previously published (DAL PUPO *et al.* 2019). (B) Flow cytometry analysis of the cryptococcal isolates after capsule staining with mAb 18B7. At least 5000 cells were analyzed for each isolate. Results are presented as average values of fluorescence intensity and are illustrative of two independent analyses producing similar results. R265 and H99 are standard cryptococcal isolates that were used as reference in this assay. Data for the Northern Brazil isolates were obtained from (DAL PUPO *et al.* 2019).

On the basis of the visual perception that antibody recognition of the capsule was variable, we measured the indices of fluorescence intensity after incubation of each isolate with the GXM-binding antibody by flow cytometry (Figure 8B). Using the standard isolates H99 and R265 as reference strains, this analysis confirmed both highly reactive strains and poorly reactive isolates, supporting the notion that surface GXM is highly diverse in *Cryptococcus*. Although *C. gattii* and *C. deuterogattii* isolates were predominantly less capsulated than *C. neoformans* (t student test *P* value <0.05), we did not observe any statistical difference between the *C. neoformans* subclades.

We also analyzed the concentration of polysaccharide in culture supernatants of each isolate (Figure S4). Detection of extracellular and surface-associated GXM was strongly correlated (Figure S4), supporting the notion that cryptococcal isolates are highly variable in their ability to form GXM-containing capsules and to export polysaccharide.

We also examined melanin production on L-Dopa medium. We observed a variable phenotype among the Brazilian isolates, with *C. gattii* and *C. deuterogattii* isolates displaying lower melanin production (Figure 9). There was no obvious correlation between melanin production among subclades, although strains isolated from bird droppings appear to produce more melanin than other environmental or clinical isolates.

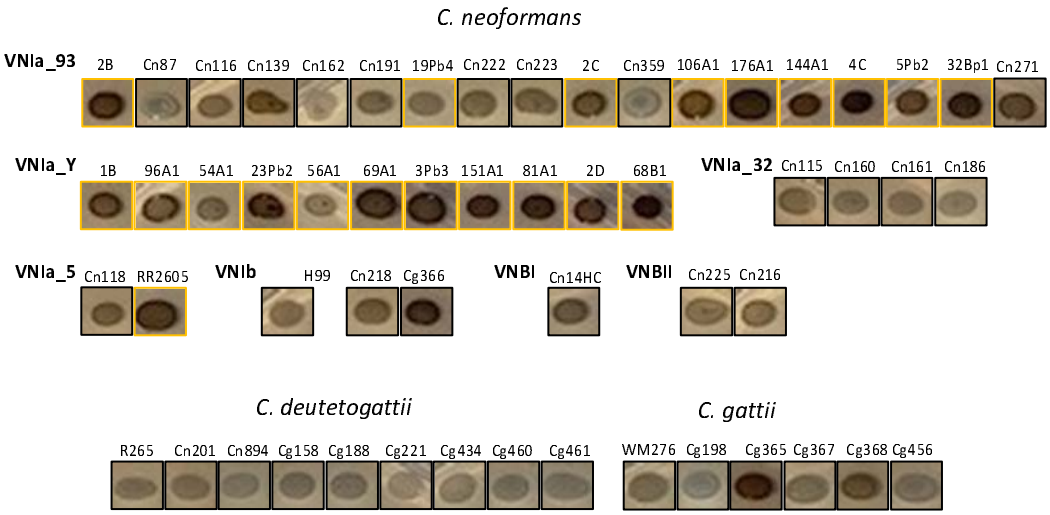


Figure 9. Melanin production of Brazilian isolates as estimated on L-Dopa medium after 72 h of incubation. Strains isolated from bird dropping are indicated by a yellow box.

Lastly, we examined production of TCs. *C. neoformans* and *C. gattii* cells can undergo an unusual transition in the host lung from the typical size of 5 to 7 µm to between 10 µm and 100 µm), a phenomenon known as TCs, which are known to be highly polyploid (ZARAGOZA AND NIELSEN 2013). TCs can also be induced in vitro using three different approaches that are currently known (DAMBUZA *et al.* 2018; HOMMEL *et al.* 2018; TREVIJANO-CONTADOR *et al.* 2018). Here, we followed the protocol described by Dambuza et al. (2018) to study whether Brazilian *Cryptococcus* strains produce TCs. In our study, *C. neoformans* H99 formed nearly 17% TCs, aligning with previously published findings (DAMBUZA *et al.* 2018). Approximately 49% of Brazilian *Cryptococcus* strains produced TCs (defined here as cells with a size >10 µm) (Figure 10, Table S4). Around 24% of Brazilian *Cryptococcus* strains generated more TCs than *C. neoformans* H99 (Figure 10, Table S4). Interestingly, and in contrast to a previous study using the same protocol, all Brazilian *C. gattii* and *C. deuterogatti* strain tested formed TCs (Figure 10, Table S4). Actually, the highest percentage of TCs (97.33%) was produced by the *C. deuterogattii* strain Cn894 (Figure 10, Table S4).

In order to address whether cells that formed more TCs than H99 are naturally larger, we compared the size of these cells before and after the titanization induction. The mean size

of the cells of Brazilian *Cryptococcus* strains varied between 4.18 to 5.70 µm before and 6.85 to 14.19 µm after cultivation in TC-inducing conditions, proving that the titanization induction was responsible for the increase in cell size (Table S5). We did not observe any link between subclade and the ability of the corresponding strain to undergo this phenotypic change.

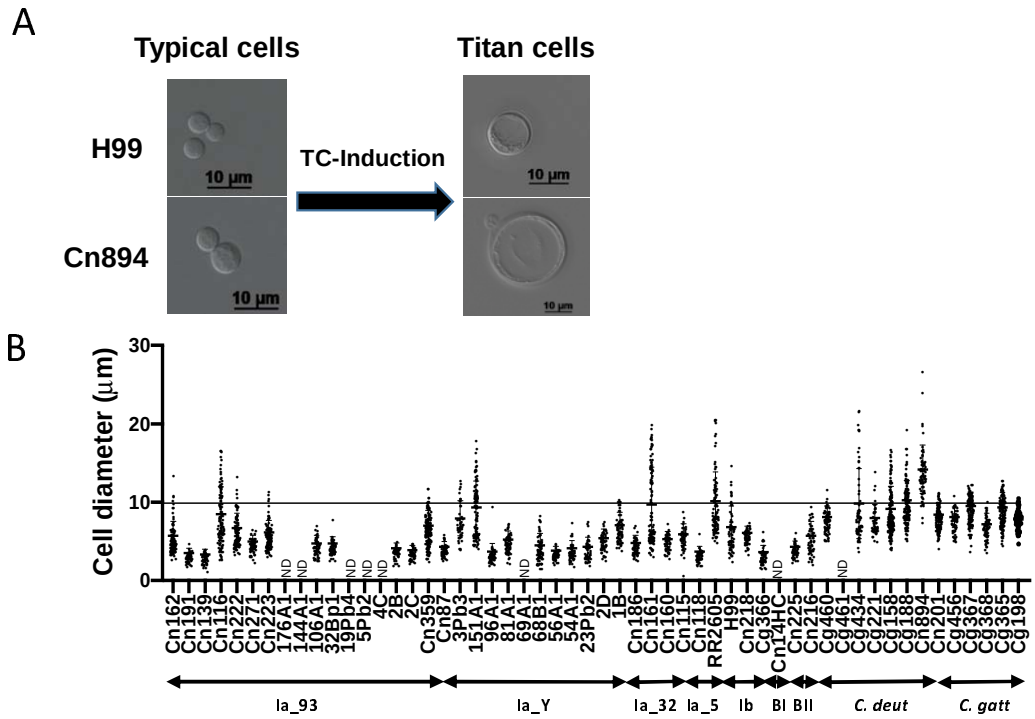


Figure 10. Titanization assay. (A) Example of Titan cells obtained from the *C. neoformans* reference strain H99 and the *C. deuterogattii* strain Cn894. (B) Cell diameter after titanization induction in Brazilian isolates. Cryptococcus strains were subjected to TC induction in PBS-HI-FCS. Cell diameter> 10 µm were considered as TC. ND: not determined.

Overall, this analysis revealed spectacular phenotypic variability within the Brazilian isolates, although no association was detected between one clade and any of these phenotypic traits.

**Discussion.**

Population genomics studies have resulted in a model in which clonal reproduction has shaped the global population structure of *C. neoformans* isolates, which are mostly of the VNI clade and of the *MATα* sexual type (CUOMO *et al.* 2018). These genome sequence analyses have also identified several VNI subclades with specific geographical distribution (ASHTON *et al.* 2019). Currently, little is known about *Cryptococcus* species diversity in South America because only a few isolates have been sequenced (RHODES *et al.* 2017b). In the present study, we analyzed the largest South American genome collection studied to date. As expected, most of the Brazilian isolates belonged to the VNI clade. Our analysis revealed that the VNI Brazilian *C. neoformans* population structure shares many features with the African population. For instance, VNI_Y isolates that were previously only reported in Africa were also prominent within this set of South America strains. As in Africa, Brazilian VNIa_5 isolates were rare; in contrast, VNIa_5 isolates represent one of the largest subclades within Asian isolates (ASHTON *et al.* 2019). A detailed analysis of the different VNIa subclade population structures further supported the hypothesis of repeated and privileged exchanges from African to South American strains. Thus, South American isolates do not form an independent clade or subclade but rather are scattered within nearly all global subclades, indicating repeated transport. Although we observed a perfect clustering of Brazilian isolates within the VNIa_Y and VNIa_32 subclades—possibly from an ancient importation followed by independent evolution of the ancestral strain—some VNIa-93 isolates clustered with the other global isolates, suggesting independent and possibly more recent importations.

A similar pattern was observed with the VNB strains. Two of the Brazilian strains were positioned close to the roots of the VNB branches, as previously observed for two previously sequenced Brazilian isolates (RHODES *et al.* 2017b). However, the third strain clustered within the other VNB African isolates, suggesting a more recent intercontinental exchange.

This study exemplified the impact of rapidly evolving strains on the *C. neoformans* population structure. Mutator phenotypes have already been observed in natural *C. neoformans* and *C. gattii* isolates and have been shown to impact the dynamics of strain evolution, phenotypic diversity, and drug resistance (BILLMYRE *et al.* 2017; BILLMYRE *et al.* 2020). A *msh2*-associated transient mutator phenotype is thought to be responsible for the rapid adaptation and evolution of virulence in the VGIIa Pacific Northwest outbreak strain (KIDD *et al.* 2004; BILLMYRE *et al.* 2014). Here, the VNBI isolate CnH14C displayed a mutator phenotype, albeit less pronounced than the previously described *C. neoformans Msh2Δ*, *mlh1Δ*, and *pms1Δ* mutant strains (BOYCE *et al.* 2017). Accordingly, we did not identify nonsense mutations in any of these genes in the CnH14C isolate. However, *PMS1*- and *RAD5*-specific alleles in CnH14C might suggest a causal relationship. In fact, *RAD5* has been recently identified as regulating mutation rates in a quantitative trait locus analysis in *S. cerevisiae* (GOU *et al.* 2019), and a specific *RAD5* mutation has also been identified in a rapidly evolved *C. neoformans* recurrent clinical isolate (RHODES *et al.* 2017a).

However, in contrast to what has been observed in some African isolates, we did not identify any hybrid strains within this collection of Brazilian isolates. As previously reported (MATSUMOTO *et al.* 2007; ANDRADE-SILVA *et al.* 2018), none of these strains were *MAT***a**. Nevertheless, our model of multiple intercontinental transport of African strains to South America and the proportion of *MAT***a** strain within the VNB strains in Africa (LITVINTSEVA *et al.* 2007; LITVINTSEVA *et al.* 2011; LITVINTSEVA AND MITCHELL 2012) predict that additional sampling will probably identify such strains.

MLST and genome sequence analysis identified South America, and in particular Brazil, as the major source of the global genetic diversity of the *C. gattii* complex, especially within the VGII and VGIII lineages (BILLMYRE *et al.* 2014; SOUTO *et al.* 2016; BARCELLOS *et al.* 2018; VILAS-BÔAS *et al.* 2020). This is associated with great phenotypic diversity within the Brazilian isolates (SILVA *et al.* 2012; BARCELLOS *et al.* 2018). Similarly, genotypic and phenotypic analyses of Brazilian *C.*

*neoformans* strains, including the analysis in the present study, have revealed great diversity within South American isolates (FERREIRA-PAIM *et al.* 2017; ANDRADE-SILVA *et al.* 2018; DAL PUPO *et al.* 2019; DE SOUSA *et al.* 2020). Nevertheless, our data suggest that Brazil is probably not an important source of global diversity of *C. neoformans* isolates. Rather, our findings support the model in which this diversity is mostly imported from Africa through repeated intercontinental transport of *C. neoformans* isolates to South America.

Our studies continue the investigation of *Cryptococcus* species global diversity and emphasize the importance of understanding the evolution of fungal pathogens. Further studies with additional isolates from Brazil and other countries in South America will help us to clarify many aspects of population genetics of this important fungal pathogen.

**Acknowledgments**

M.L.R. is currently on leave from the position of associate professor at the Microbiology Institute of the Federal University of Rio de Janeiro, Brazil. M.L.R., G.J., and G.H.G. were supported by a Tripartite USP-Fiocruz-Pasteur grant. FCGR was financed in part by a scholarship from the Coordenação de Aperfeiçoamento de Pessoal de Nível Superior (CAPES, Brazil, Finance Code 001).

References


Alanio, A., 2020 Dormancy in *Cryptococcus neoformans*: 60 years of accumulating evidence. The Journal of Clinical Investigation 130: 3353-3360.

Aminnejad, M., M. Diaz, M. Arabatzis, E. Castaneda, M. Lazera *et al.*, 2012 Identification of novel hybrids between *Cryptococcus neoformans* var. *grubii* VNI and *Cryptococcus gattii* VGII. Mycopathologia 173.

Andrade-Silva, L. E., K. Ferreira-Paim, T. B. Ferreira, A. Vilas-Boas, D. J. Mora *et al.*, 2018 Genotypic analysis of clinical and environmental Cryptococcus neoformans isolates from Brazil reveals the presence of VNB isolates and a correlation with biological factors. PLOS ONE 13: e0193237.

Ashton, P. M., L. T. Thanh, P. H. Trieu, D. Van Anh, N. M. Trinh *et al.*, 2019 Three phylogenetic groups have driven the recent population expansion of Cryptococcus neoformans. Nature Communications 10: 2035.

Barcellos, V. A., L. M. S. Martins, A. C. L. Fontes, J. C. V. Reuwsaat, E. D. Squizani *et al.*, 2018 Genotypic and Phenotypic Diversity of Cryptococcus gattii VGII Clinical Isolates and Its Impact on Virulence. Frontiers in microbiology 9: 132-132.

Basenko, E. Y., J. A. Pulman, A. Shanmugasundram, O. S. Harb, K. Crouch *et al.*, 2018 FungiDB: An integrated bioinformatic resource for Fungi and Oomycetes. Journal of Fungi 4: 39.

Billmyre, R. B., S. Applen Clancey, L. X. Li, T. L. Doering and J. Heitman, 2020 5-fluorocytosine resistance is associated with hypermutation and alterations in capsule biosynthesis in Cryptococcus. Nature Communications 11: 127.

Billmyre, R. B., S. A. Clancey and J. Heitman, 2017 Natural mismatch repair mutations mediate phenotypic diversity and drug resistance in Cryptococcus deuterogattii. eLife 6: e28802.

Billmyre, R. B., D. Croll, W. Li, P. Mieczkowski, D. A. Carter *et al.*, 2014 Highly recombinant VGII *Cryptococcus gattii* population develops clonal outbreak clusters through both sexual macroevolution and asexual microevolution. mBio 5: e01494-01414.

Boekhout, T., B. Theelen, M. Diaz, J. W. Fell, W. C. J. Hop *et al.*, 2001 Hybrid genotypes in the pathogenic yeast Cryptococcus neoformans. Microbiology 147: 891-907.

Bovers, M., F. Hagen, E. E. Kurumae, H. L. Hoogveld, F. Dromer *et al.*, 2008 AIDS patient death caused by novel *Cryptococcus neoformans* x *C. gattii* hybrid. Emerging Infectious Diseases 14: 1105-1108.

Boyce, K. J., Y. Wang, S. Verma, V. P. S. Shakya, C. Xue *et al.*, 2017 Mismatch repair of DNA replication errors contributes to microevolution in the pathogenic fungus *Cryptococcus neoformans*. mBio 8: e00595-00517.

Bui, T., X. Lin, R. Malik, J. Heitman and D. Carter, 2008 Isolates from *Cryptococcus neoformans* from infected animals reveal genetics exchange in unisexual, $\alpha$ mating type population. Eukaryotic Cell 7: 1771-1780.

Casadevall, A., J. Mukherjee, S. J. N. Devi, R. Schneerson, J. B. Robbins *et al.*, 1992 Antibodies Elicited by a Cryptococcus neoformans-Tetanus Toxoid Conjugate Vaccine Have the Same Specificity as Those Elicited in Infection. The Journal of Infectious Diseases 165: 1086-1093.

Cuomo, C. A., J. Rhodes and C. A. Desjardins, 2018 Advances in Cryptococcus genomics: insights into the evolution of pathogenesis. Memórias do Instituto Oswaldo Cruz 113.

Dal Pupo, H. D., B. A. G. Sena, F. C. G. Reis, L. Machado, S. T. Fortes *et al.*, 2019 Polysaccharide diversity in VNI isolates of Cryptococcus neoformans from Roraima, Northern Brazil. Fungal Biology 123: 699-708.

Dambuza, I. M., T. Drake, A. Chapuis, X. Zhou, J. Correia *et al.*, 2018 The Cryptococcus neoformans Titan cell is an inducible and regulated morphotype underlying pathogenesis. PLOS Pathogens 14: e1006978.

de Sousa, H. R., G. P. de Oliveira, S. de Oliveira Frazão, K. C. de Melo Gorgonha, C. P. Rosa *et al.*, 2020 Faster *Cryptococcus* melanization increases virulence in experimental and human cryptococcosis. bioRxiv: 2020.2007.2029.222794.

Desjardins, C. A., C. Giamberardino, S. M. Sykes, C.-H. Yu, J. L. Tenor *et al.*, 2017 Population genomics and the evolution of virulence in the fungal pathogen *Cryptococcus neoformans*. Genome research 27: 1207-1219.

Engelthaler, D. M., N. D. Hicks, J. D. Gillece, C. C. Roe, J. M. Schupp *et al.*, 2014 *Cryptococcus gattii* in North American Pacific Northwest: Whole-Population Genome Analysis Provides Insights into Species Evolution and Dispersal. mBio 5: e01464-01414.

Ergin, Ç., M. Şengül, L. Aksoy, A. Döğen, S. Sun *et al.*, 2019 *Cryptococcus neoformans* recovered from olive trees (*Olea europaea*) in Turkey reveal allopatry with African and South American lineages. Frontiers in Cellular and Infection Microbiology 9.

Farrer, R. A., M. Chang, M. J. Davis, L. van Dorp, D.-H. Yang *et al.*, 2019 A new lineage of *Cryptococcus gattii* (VGV) discovered in the central Zambezian Miombo Woodlands. mBio 10: e02306-02319.

Ferreira-Paim, K., L. Andrade-Silva, F. M. Fonseca, T. B. Ferreira, D. J. Mora *et al.*, 2017 MLST-Based Population Genetic Analysis in a Global Context Reveals Clonality amongst Cryptococcus neoformans var. grubii VNI Isolates from HIV Patients in Southeastern Brazil. PLOS Neglected Tropical Diseases 11: e0005223.

Foster, P. L., 2006 Methods for determining spontaneous mutation rates. Methods in enzymology 409: 195-213.

Garcia-Hermoso, D., G. Janbon and F. Dromer, 1999 Epidemiological evidence for dormant *Cryptococcus neoformans* infection. Journal of Clinical Microbiology 37: 3204-3209.

Gillet-Markowska, A., G. Louvel and G. Fischer, 2015 *bz-rates*: A Web Tool to Estimate Mutation Rates from Fluctuation Analysis. G3: Genes|Genomes|Genetics 5: 2323.

Gonzalez-Hilarion, S., D. Paulet, K.-T. Lee, C.-C. Hon, P. Lechat *et al.*, 2016 Intron retention-dependent gene regulation in *Cryptococcus neoformans*. Scientific Reports 6: 32252.

Gou, L., J. S. Bloom and L. Kruglyak, 2019 The Genetic Basis of Mutation Rate Variation in Yeast. Genetics 211: 731-740.

Guindon, S., J.-F. Dufayard, V. Lefort, M. Anisimova, W. Hordijk *et al.*, 2010 New Algorithms and Methods to Estimate Maximum-Likelihood Phylogenies: Assessing the Performance of PhyML 3.0. Systematic Biology 59: 307-321.

Hagen, F., K. Khayhan, B. Theelen, A. Kolecka, I. Polacheck *et al.*, 2015 Recognition of seven species in the Cryptococcus gattii/Cryptococcus neoformans species complex. Fungal Genetics and Biology 78: 16-48.

Hommel, B., L. Mukaremera, R. J. B. Cordero, C. Coelho, C. A. Desjardins *et al.*, 2018 Titan cells formation in Cryptococcus neoformans is finely tuned by environmental conditions and modulated by positive and negative genetic regulators. PLOS Pathogens 14: e1006982.

Institute, C. L. S., 2017 Reference method for broth dilution antifungal susceptibility testing of yeasts; approved standard, document document M27-A3 in *National Committee for Clinical Laboratory Standards*.

Janbon, G., K. L. Ormerod, D. Paulet, E. J. Byrnes III, G. Chatterjee *et al.*, 2014 Analysis of the genome and transcriptome of *Cryptococcus neoformans* var. *grubii* reveals complex RNA expression and microevolution leading to virulence attenuation. PLoS Genetics 10: e1004261.

Janbon, G., J. Quintin, F. Lanternier and C. d'Enfert, 2019 Studying fungal pathogens of humans and fungal infections: fungal diversity and diversity of approaches. Genes & Immunity 20: 403-414.

Johnston, S. A., K. Voelz and R. C. May, 2016 Cryptococcus neoformans Thermotolerance to Avian Body Temperature Is Sufficient For Extracellular Growth But Not Intracellular Survival In Macrophages. Scientific Reports 6: 20977.

Kidd, S. E., F. Hagen, R. L. Tscharke, M. Huynh, K. H. Bartlett *et al.*, 2004 A rare genotype of *Cryptococcus gattii* caused the cryptococcosis outbreak on Vancouver Island (British Columbia, Canada). Proceeding of the National Academy of Sciences of the USA 101: 17258-17263.

Kwon-Chung, K. J., and J. E. Bennett, 1978 Distribution of a and $\alpha$ mating types of *Cryptococcus neoformans* among natural and clinical isolates. American Journal of Epidemiology 108: 337-340.

Kwon-Chung, K. J., J. A. Fraser, T. L. Doering, Z. Wang, G. Janbon *et al.*, 2014 *Cryptococcus neoformans* and *Cryptococcus gattii*, the etiologic agents of cryptococcosis. Cold Spring Harb Perspect Med 4: a019760.

Li, H., 2018 Minimap2: pairwise alignment for nucleotide sequences. Bioinformatics 34: 3094-3100.

Li, H., B. Handsaker, A. Wysoker, T. Fennell, J. Ruan *et al.*, 2009 The Sequence Alignment/Map format and SAMtools. Bioinformatics (Oxford, England) 25: 2078-2079.

Lin, X., and J. Heitman, 2006 The biology of the *Cryptococcus neoformans* species complex. Annual Review of Microbiology 60: 69-105.

Lin, X., S. Patel, A. P. Litvintseva, A. Floyd, T. G. Mitchell *et al.*, 2009 Diploids in the *Cryptococcus neoformans* serotype A population homozygous for the alpha mating type originate via unisexual mating. PLoS Pathog 5: e1000283.

Litvintseva, A. P., I. Carbone, J. Rossouw, R. Thakur, N. P. Govender *et al.*, 2011 Evidence that the human pathogenic fungus *Cryptococcus neoformans* var. grubii may have evolved in Africa. PloS One 6: e19688.

Litvintseva, A. P., L. Kestenbaum, R. Vilgalys and T. G. Mitchell, 2005 Comparative analysis of environmental and clinical populations of *Cryptococcus neoformans*. Journal of Clinical Microbiology 43: 556-564.

Litvintseva, A. P., X. Lin, I. Templeton, J. Heitman and T. G. Mitchell, 2007 Many Globally Isolated AD Hybrid Strains of Cryptococcus neoformans Originated in Africa. PLOS Pathogens 3: e114.

Litvintseva, A. P., R. E. Marra, K. Nielsen, J. Heitman, R. Vilgalys *et al.*, 2003 Evidence of sexual recombination among *Cryptococcus neoformans* serotype A isolates in sub-Saharan Africa. Eukaryotic Cell 2: 1162-1168.

Litvintseva, A. P., and T. G. Mitchell, 2012 Population genetic analyses reveal the African origin and strain variation of *Cryptococcus neoformans* var. *grubii*. PLoS Pathog 2012: e1002495.

Loftus, B., E. Fung, P. Roncaglia, D. Rowley, P. Amedeo *et al.*, 2005 The genome and transcriptome of *Cryptococcus neoformans*, a basidiomycetous fungal pathogen of humans. Science 307: 1321-1324.

Matsumoto, M. T., A. M. Fusco-Almeida, L. C. Baeza, M. d. S. C. Melhem and M. J. S. Medes-Giannini, 2007 Genotyping, serotyping and determination of mating-type of Cryptococcus neoformans clinical isolates from São Paulo State, Brazil. Revista do Instituto de Medicina Tropical de São Paulo 49: 41-47.

Meyer, W., D. M. Aanensen, T. Boekhout, M. Cogliati, M. R. Diaz *et al.*, 2009a Consensus multi-locus sequence typing scheme for Cryptococcus neoformans and Cryptococcus gattii. Medical mycology 47: 561-570.

Meyer, W., D. M. Aanensen, T. Boekhout, M. Cogliati, M. R. Diaz *et al.*, 2009b Consensus multi-locus sequence typing scheme for *Cryptococcus neoformans* and *Cryptococcus gattii*. Medical Mycology 57: 561-570.

Raj, A., M. Stephens and J. K. Pritchard, 2014 fastSTRUCTURE: Variational Inference of Population Structure in Large SNP Data Sets. Genetics 197: 573.

Rajasingham, R., R. M. Smith, B. J. Park, J. N. Jarvis, N. P. Govender *et al.*, 2017 Global burden of disease of HIV-associated cryptococcal meningitis: an updated analysis. The Lancet Infectious Diseases 17: 873-881.

Rhodes, J., M. A. Beale, M. Vanhove, J. N. Jarvis, S. Kannambath *et al.*, 2017a A Population Genomics Approach to Assessing the Genetic Basis of Within-Host Microevolution Underlying Recurrent Cryptococcal Meningitis Infection. G3: Genes|Genomes|Genetics 7: 1165.

Rhodes, J., C. A. Desjardins, S. M. Sykes, M. A. Beale, M. Vanhove *et al.*, 2017b Tracing genetic exchange and biogeography of *Cryptococcus neoformans* var. *grubii* at the global population level. Genetics: 10.1534/genetics.1117.203836.

Ruma, P., S. C. A. Chen, T. C. Sorrel and A. G. Brownlee, 1996 Characterization of Cryptococcus neoformans by random DNA amplification. Letters in Applied Microbiology 23: 312-316.

Silva, D. C., M. A. Martins, M. W. Szeszs, L. X. Bonfietti, D. Matos *et al.*, 2012 Susceptibility to antifungal agents and genotypes of Brazilian clinical and environmental Cryptococcus gattii strains. Diagnostic Microbiology and Infectious Disease 72: 332-339.

Souto, A. C. P., L. X. Bonfietti, K. Ferreira-Paim, L. Trilles, M. Martins *et al.*, 2016 Population Genetic Analysis Reveals a High Genetic Diversity in the Brazilian Cryptococcus gattii VGII Population and Shifts the Global Origin from the Amazon Rainforest to the Semi-arid Desert in the Northeast of Brazil. PLoS neglected tropical diseases 10: e0004885-e0004885.

Trevijano-Contador, N., H. C. de Oliveira, R. García-Rodas, S. A. Rossi, I. Llorente *et al.*, 2018 Cryptococcus neoformans can form titan-like cells in vitro in response to multiple signals. PLOS Pathogens 14: e1007007.

Vanhove, M., M. A. Beale, J. Rhodes, D. Chanda, S. Lakhi *et al.*, 2017 Genomic epidemiology of Cryptococcus yeasts identifies adaptation to environmental niches underpinning infection across an African HIV/AIDS cohort. Molecular ecology 26: 1991-2005.

Vilas-Bôas, A. M., L. E. Andrade-Silva, K. Ferreira-Paim, D. J. Mora, T. B. Ferreira *et al.*, 2020 High genetic variability of clinical and environmental Cryptococcus gattii isolates from Brazil. Medical Mycology 58: 1126-1137.

Yadav, V., S. Sun, R. B. Billmyre, B. C. Thimmappa, T. Shea *et al.*, 2018 RNAi is a critical determinant of centromere evolution in closely related fungi. Proceeding of the National Academy of Sciences of the USA 115: 3108.

Zaragoza, O., and K. Nielsen, 2013 Titan cells in Cryptococcus neoformans: Cells with a giant impact. Current Opinion in Microbiology 16: 409-413.